



**ROMANIAN ACADEMY**  
**School of Advanced Studies of the Romanian Academy**  
**Institute of Biochemistry of the Romanian Academy**

## **PHD THESIS SUMMARY**

**Development of an anti-B7-H3 Cytotoxic Affibody with potential in  
Acute Myeloid Leukemia immunotherapy**

**PHD COORDINATOR:**  
**CSI Prof. Dr. Ștefan-Eugen Szedlacsek**

**PHD CANDIDATE:**  
**Vasilescu Andrei-Mihai**

# TABLE OF CONTENTS

ABBREVIATIONS.....	3
<b>I. INTRODUCTION.....</b>	<b>4</b>
Hypothesis.....	6
Objectives.....	6
<b>II. PART I. THEORETICAL ASPECTS.....</b>	<b>7</b>
1. CD276 (B7-H3).....	7
1.1. Structure and Isoforms.....	7
1.2. Involvement in Immune System Regulation.....	8
1.3. Implications in Cancer.....	9
1.4. B7-H3 as a Potential Biomarker in Acute Myeloid Leukemia.....	11
2. SMALL MOLECULAR VEHICLES DIRECTED AGAINST CANCER BIOMARKERS.....	13
2.1. DNA INHIBITORS.....	13
2.2. AFFIBODIES.....	14
2.2.1. Structure and Properties.....	14
2.2.2. Function as Antigen Binders.....	15
2.2.3. Affibodies as Delivery Vehicles for Imaging and Therapeutics.....	17
2.2.4. Anti-B7-H3 Affibodies.....	21
3. CYTOTOXIC PEPTIDES AGAINST CANCER.....	22
3.1. Efficiency and Side Effects.....	22
3.2. Magainin-2 as a Specific Anti-Tumoral Agent.....	23
<b>PART II. EXPERIMENTAL SECTION.....</b>	<b>26</b>
1. INTRODUCTION.....	26
2. MATERIALS AND METHODS.....	27
2.1. Expression Plasmid.....	27
2.2. Bacterial Cloning of the pET-19b expression plasmid.....	28
2.3. Cell Lines.....	28

2.4. Expression and Purification of 6xHis-SUMO-Aff-MAG2.....	29
2.5. NanoLC-MS/MS analysis of the purified Aff-MAG2 construct and evaluation of a hypothetical cleavage site.....	32
2.6. MTS Assay.....	33
2.7. Flow Cytometry.....	33
2.8. Western Blot.....	35
2.9. Data Analysis and Statistics.....	36
3. RESULTS.....	37
3.1. Design of a Novel Recombinant Affibody Targeting B7-H3 Fused to Magainin-2....	37
3.2. Design and Cloning of the Expression Vector for 6xHis-SUMO-Aff-MAG2.....	39
3.3. Aff-MAG2 was Expressed and Purified from E. coli with high yields.....	41
3.4. Amino Acid Sequence Confirmation of the purified Aff-MAG2 by NanoLC-MS/MS Analysis.....	46
3.5. Evaluation of Aff-MAG2 Stability and potential Degradation sites.....	47
3.6. Inhibitory Effect Displayed by Aff-MAG2 on Acute Myeloid Leukemia cells.....	50
3.7. Aff-MAG2 Causes intense Necrosis and Apoptosis in AML cells.....	53
3.8. AML cells Suffer Proliferation Decrease upon treatment with Aff-MAG2.....	59
4. DISCUSSION.....	62
Limitations.....	65
Perspectives.....	65
<b>III. CONCLUSION.....</b>	<b>66</b>
ACKNOWLEDGEMENTS.....	67
LIST OF PUBLICATIONS.....	68
REFERENCES.....	69

# I. INTRODUCTION

Acute Myeloid Leukemia (AML) comprises a heterogeneous group of malignant hematological disorders characterized by rapid proliferation of abnormal myeloid precursors, metastasis, high resistance to chemotherapy and radiotherapy and poor long-term survival rates (Fan et al., 2023). Compounding these dangerous properties is the fact that AML cells can evade therapeutic stress by residing in the bone marrow niche, which contributes to multidrug resistance and increases relapse risk in patients (Wittwer et al., 2017). Therefore, AML remains a life-threatening disease that requires new and effective therapeutic strategies. This PhD thesis is composed of two main parts. **PART I.** presents the scientific background and recent discoveries that provided the rationale and the need for the experimental study described in **PART II.**, which represents the personal contributions made by the thesis author.

## Hypothesis

The hypothesis of this PhD thesis is: A rationally-designed Anti-B7-H3 Affibody-Magainin-2 recombinant construct can be produced from a prokaryotic expression system and it causes necrosis, apoptosis and inhibited proliferation in Acute Myeloid Leukemia representative cells.

## Objectives

This study involves the following objectives:

- Design of the cytotoxic B7-H3-targeting protein Aff-MAG2
- Expression in *E. coli*, purification of the designed recombinant protein and amino acid sequence validation of the purified conjugate
- Stability evaluation of the obtained construct
- Determination of Aff-MAG2 IC<sub>50</sub> against AML representative cells
- Evaluation of Aff-MAG2 necrotic and apoptotic effects on model cells for AML
- Effects of the cytotoxic conjugate on the proliferation of representative cells for AML

## II. PART I. THEORETICAL ASPECTS

### 1. CD276 (B7-H3)

#### **B7-H3 as a Potential Biomarker in Acute Myeloid Leukemia**

Although B7-H3 mRNA is expressed almost ubiquitously in normal adult human cells, owing to a strict post-transcriptional and post-translational regulation, the protein is almost non-existent in the healthy adult organism (Guo et al., 2025). In contrast, as previously stated, B7-H3 is highly expressed in cancer cells of many different origins, including in AML cells. Of much greater importance, however, is the fact that overexpression of B7-H3 in AML patients correlates with a highly significant decrease in overall survival over time, as seen in data from The Cancer Genome Atlas (TCGA) database analyzed in this study (**Figure 1**). Given all these data about the crucial importance of B7-H3 overexpression that is specific to AML cells, B7-H3 is a powerful potential biomarker for diagnostic and response to treatment in AML. The important status of B7-H3 in AML was also recognized in previous studies (Fan et al., 2023; Tan & Zhao, 2024). For these reasons, the author considers that B7-H3 represents an excellent target for directed personalized therapy in AML with likely no serious side effects. This statement is further supported by a multitude of pre-clinical studies on AML that utilized different strategies to target B7-H3 with high rates of success (Stefańczyk et al., 2024; Tyagi et al., 2022; Zhang et al., 2020), as well as by promising ongoing clinical trials in the same context (Guo et al., 2025). Therefore, the author chose **B7-H3 in AML** as the therapeutic target for this PhD thesis.

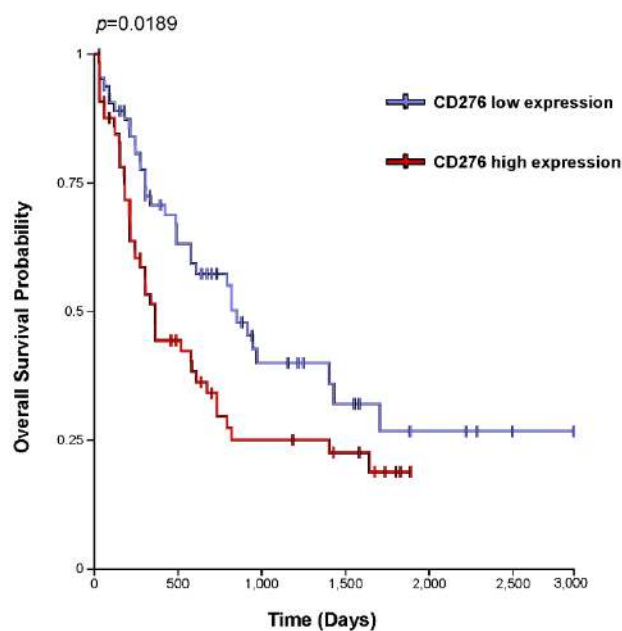


**Figure 1.** Kaplan-Meier overall survival probability for patients with AML, over the course of ~8 years from diagnostic. Comparison between survival of patients with low gene expression of B7-H3 (CD276) vs. high gene expression of B7-H3, analyzed at the mRNA level through RNA-Seq of clinical samples from the TCGA database. The log-rank test was employed to determine statistical significance.  $p < 0.05$  is considered statistically significant.

## 2. SMALL MOLECULAR VEHICLES DIRECTED AGAINST CANCER BIOMARKERS

### Anti-B7-H3 Affibodies

For this PhD thesis, the amino acid sequence of the highly promising affibody molecule **SYNT-179** was used, which was matured, extensively characterized and validated by Oroujeni et al. in 2023. By using a comprehensive methodology, they demonstrated high specificity of this affibody towards B7-H3 *in vitro* (radioactive labeling) and *in vivo* (ovarian cancer xenografted mice imaged with nanoSPECT/CT) and an excellent affinity of  $K_{D1} = 0.028 \pm 0.001$  nM for the rarest epitope of B7-H3 and  $K_{D2} = 8.2 \pm 0.5$  nM for the most abundant epitope, as measured by LigandTracer (Oroujeni et al., 2023). This more robust methodology and LigandTracer determinations reveal the fact that SYNT-179 is vastly

superior to its parent molecule, AC12, which, according to these more precise measurements, has a  $K_{D2}$  of only  $68.8 \pm 7.4$  nM. The same group proved again in 2025, on human ovarian cancer xenografted mice models that SYNT-179 is a formidable candidate for imaging diagnostics of B7-H3-expressing cancers (Tolmachev et al., 2025). Taken together, these data make SYNT-179 the best anti-B7-H3 affibody to date and the perfect candidate for the present study of a new potential therapeutic for B7-H3-positive AML.

### **3. CYTOTOXIC PEPTIDES AGAINST CANCER**

#### **Magainin-2 as a Specific Anti-Tumoral Agent**

Magainin-2 (MAG2) is a 23-amino acid simple, cationic peptide that has no post-translational modifications and adopts the 3D structure of an alpha-helix (Zasloff, 1987). This simple structure gives it important advantages, such as stability and high solubility, but the most crucial one is that it allows its expression and production in bacteria quickly and cheaply. In fact, Ramos et al. (2013) managed to produce MAG2 in *E. coli* and proved it was soluble and functional. Certain techniques exist that allow prokaryote expression of this membranolytic peptide that were also employed in the present study, yet they are described later, in the DISCUSSION section.

Besides its lethal effects on a wide array of bacteria and even fungi and protozoa (Zasloff, 1987), MAG2 has demonstrated strong activity against cancer cells originating from many different malignancies (Cruciani et al., 1991; Ohsaki et al., 1992). For example, MAG2 was effective in selectively killing representative human bladder cancer cells *in vitro*, causing necrosis and decreased cell proliferation (Lehmann et al., 2006). Furthermore, *in vivo* experiments on mice with ascites tumors xenografted from various human cancer cell lines, including some representative of leukemia, showed significant malignant cell inhibition and a 50% longer median survival time of treated mice (Baker et al., 1993). These strong anti-tumoral effects that were demonstrated previously, both *in vitro* and *in vivo*, along with the favorable physico-chemical properties of MAG2, make it the perfect choice as the therapeutic payload of the construct developed in this PhD thesis. Taking into account all the information presented in this first part of the work, the cytotoxic recombinant construct

that was utilized in the experimental part was comprised of the **SYNT-179 Anti-B7-H3 Affibody** genetically fused to **Magainin-2** that resulted in the **Aff-MAG2** construct.

Initially, simulation and electron microscopy studies led to the idea that MAG2 kills cells by forming large pores in their plasma membrane in the toroid model (Lehmann et al., 2006; Matsuzaki, 1998). However, only recently, Pandidan and Mechler (2025) showed in a fascinating Atomic Force Microscopy (AFM) experiment that membrane destabilization caused by MAG2 is a gradual, multi-step process in which the pores are short-lived, making way, with higher MAG2 concentrations, for a more systemically destabilized wavy structure they dubbed “corduroy”. Therefore, this recent discovery was integrated into the hypothesized mechanism of action for Aff-MAG2 that is presented in **Figure 2**.

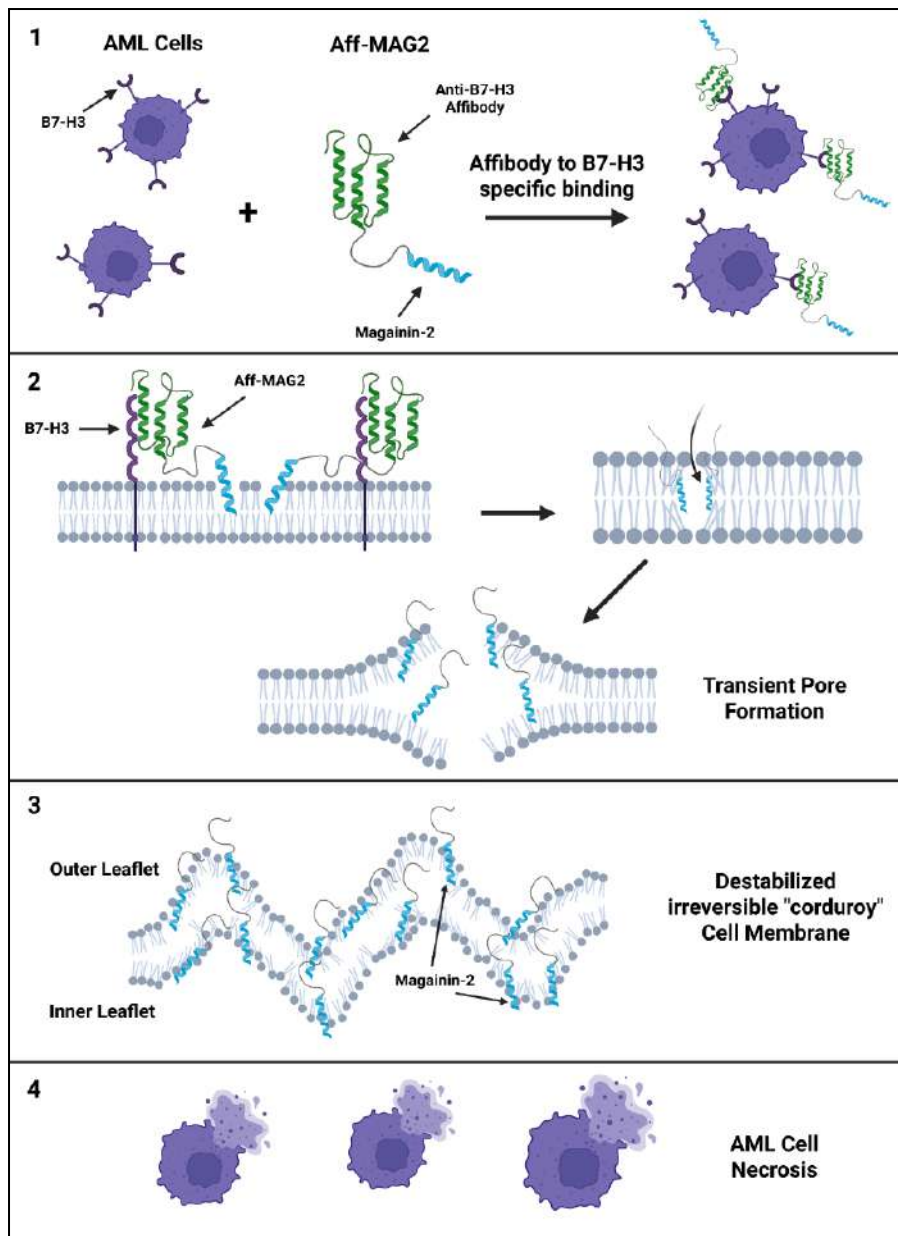


**Figure 2.** Proposed mechanism of action for the Aff-MAG2 cytotoxic construct developed in this work. **1** - Binding of Aff-MAG2 to B7-H3 expressed on the surface of AML cells, **2** - Penetration of cell membrane by Magainin-2 following the B7-H3 binding by the Affibody and subsequent transient pore formation, **3** - Irreversible stage of cell membrane destabilization after equilibration of Magainin-2 on both leaflets and formation of “corduroy” structures, **4** - Necrosis of AML cells. Created in <https://BioRender.com> by Andrei-Mihai Vasilescu.

The affibody is directed to and binds B7-H3 located on the surface of AML cells through its strong affinity to the target and effectively brings the toxic peptide MAG2 in proximity of the cell membrane. Here, the toxin penetrates the outer leaflet of the plasma membrane and through a cumulative effect created by multiple MAG2 molecules, many transient pores are formed in the membrane, followed by insertion of peptide molecules in the inner leaflet, increasing destabilization and eventually forming “corduroy” structures, a critical, unsustainable state. This results in AML cell death by necrosis. In conclusion, this developed Affibody-Drug Conjugate is hypothesized to kill B7-H3<sup>+</sup> Acute Myeloid Leukemia cells through plasma membrane lysis in a specific, targeted manner.

## PART II. EXPERIMENTAL SECTION

### 1. MATERIALS AND METHODS

A pET-19b expression plasmid vector was ordered from GenScript with the DNA sequence of the 6xHis-SUMO-Aff-MAG2 construct inserted between two unique restriction sites. As a representative cell line for AML, THP-1 (Acute monocytic leukemia monocytes) were used, from our institute's frozen stocks and RAJI cells (Burkitt lymphoma B-lymphocytes) ("ATCC: The Global Bioresource Center", 2025), as the negative control. Functional cell-based tests of the compound were employed and these were comprised of MTS assay for cell viability inhibition, flow cytometry for necrosis and apoptosis and Western blot for apoptosis and proliferation marker expression levels.

The Kaplan-Meier overall survival curves were plotted in the UCSC Xena platform, using clinical RNA-Seq B7-H3 expression data from the GDC TCGA Acute Myeloid Leukemia database. The follow-up cutoff was ~8 years. To determine statistical significance of the survival curves, the log-rank test was employed (Goldman et al., 2020). **Figure 2** was created in <https://BioRender.com> ("Scientific Image and Illustration Software | BioRender", 2025). All experiments were performed independently at least two times and at least two biological replicates were utilized. Furthermore, three technical replicates were employed where necessary. The inhibitory dose-response curves were fitted and plotted and the IC<sub>50</sub> of Aff-MAG2 was calculated in GraphPad Prism v9.3.0 (Dotmatics). An unpaired one-tailed *t*-test performed in GraphPad Prism v9.3.0 was utilized to determine statistical significance. For all statistical tests utilized,  $p \geq 0.05$  was considered as not significant, while  $p < 0.05$  was considered statistically significant.

## 2. RESULTS

### Design of a Novel Recombinant Affibody Targeting B7-H3 Fused to Magainin-2

First, the amino acid sequence of the fusion construct was designed according to established guidelines of recombinant protein rational design (Chen et al., 2013; Li, 2011; Zorko & Jerala, 2010). The design and therapeutic strategy of the compound were also based on a previous study co-authored by the thesis author (Váradi et al., 2023). As described in the recent publication by the thesis author (Vasilescu et al., 2025), the **SYNT-179** affibody was used in the construct, followed by a triple GGGGS linker and the Magainin-2 (MAG2) toxin sequence at the C-terminus. For affinity purification, a 6xHis tag was added at the N-terminus, followed by a Small Ubiquitin-related MOdifier (SUMO) tag (SMT3 from *S. cerevisiae*) for separating the tags from the final AffDC after purification (**Figure 3A**). The amino acid sequence of the affibody (SYNT-179), from N-term to C-term, is: **AEAKFAKEKINALGEIHWLPNLTYDQIKAFIAKLNDDPSQSSELLSEAKKLSE SQ**, while for MAG2 it is: **GIGKFLHSAKKFGKAFVGEIMNS**. The GGGGS linker was selected due to its proven stability, flexibility and resistance to proteolysis. Its triple repeat ensures sufficient length to prevent steric hindrance and to allow proper spatial separation of functional domains (Chen et al., 2013). The SUMO tag plays several essential roles in the design. First, it allows cleavage without leaving residual amino acids, since the SUMO protease Ulp1 (*S. cerevisiae*) specifically recognizes the SUMO domain's tertiary structure and cleaves precisely at its C-terminus, preserving the native N-terminus of the target protein (Li, 2011). This is especially important for molecules used for targeting biomarkers like the affibody. Secondly, the SUMO tag is presumed to protect against protease degradation and to attenuate the antibacterial activity of Magainin-2, which could otherwise compromise bacterial viability during expression. This protection effect could be due to electrostatic interactions between the negatively charged SUMO tag and the positively charged Magainin-2 at physiological pH (Bommarius et al., 2010). This aspect will be discussed later. Finally, the affibody, linker, toxic peptide and the SUMO tag are all very water soluble, aiding in easy recovery of the expressed construct in the bacterial lysate supernatant in high yields (Chen et al., 2013; Li, 2011; Tolmachev et al., 2025; Zasloff, 1987).

The structure of Aff-MAG2 was modeled in AlphaFold3 Server (Abramson et al., 2024) and the stable alpha-helical structures of both the anti-B7-H3 affibody and MAG2 can

be seen in **Figure 3B**, predicted with high confidence. Also, in this theoretical predicted model, there appears to be an interaction between the affibody and the toxic peptide. The implications of this possible interaction are discussed later in this paper. Other physico-chemical properties of the construct necessary for optimization of the purification procedure and subsequent experiments were calculated utilizing ProtParam from ExPASy (pI, molecular weight, protease cleavage sites) (Gasteiger et al., 2005) and SCRATCH Protein Predictor (SOLpro - solubility upon overexpression in *E. coli*) (Cheng et al., 2005).

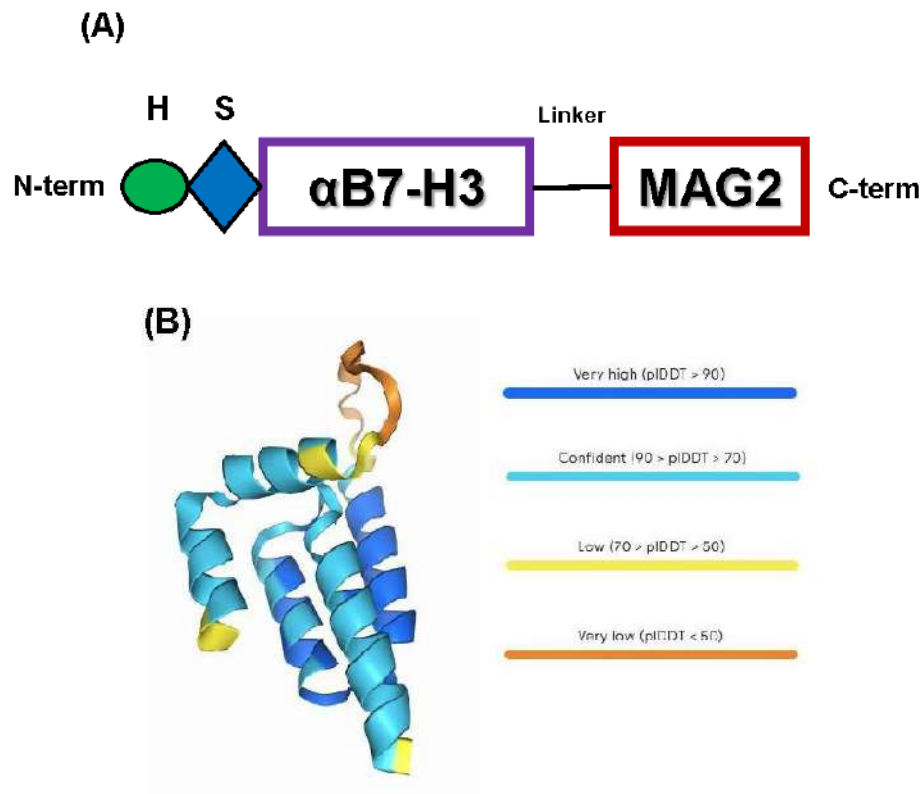


**Figure 3.** Design of the recombinant fusion protein. **(A)** Schema of the 6xHis-SUMO-Aff-MAG2 recombinant protein conjugate. **H** – 6xHis tag, **S** – SUMO tag,  **$\alpha$ B7-H3** – Anti-B7-H3 affibody, **MAG2** – Magainin-2. **(B)** AlphaFold 3 structural model of the final recombinant compound. Coincidentally, the N-terminus and the C-terminus are the yellow regions at the end of two of the alpha-helices. The protein is most likely ordered into 3 alpha-helices that succeed one another, comprising the affibody, followed by the disordered linker region and with the alpha-helix of Magainin-2 at the terminus. pLDDT - predicted local Distance Difference Test, used by AlphaFold to measure confidence of the model prediction. This figure is adapted from (Vasilescu et al., 2025), used under the CC BY 4.0 license (<https://creativecommons.org/licenses/by/4.0/>).

## Aff-MAG2 was Expressed and Purified from *E. coli* with high yields

Due to the efficient rational design of the construct, the recombinant protein was successfully expressed in *E. coli* using a slower expression rate at 18 °C, for optimal protein folding, in the described pET-19b vector and with the majority of the product in soluble form (**Figure 4A**, lane 5). Subsequently, utilizing Immobilized Metal Affinity Chromatography (IMAC), relatively pure fractions of the protein were obtained (**Figure 4B**, lanes 6-15) and as can be observed in **Figure 4B**, lane 4 (the column flowthrough), the binding to the Ni-Sepharose column was very effective. After dialysis, the combined protein fractions were taken through the last step of purification. SUMO protease was used to cleave the tags and then the final Aff-MAG2 untagged compound was separated in the supernatant using Ni-Agarose resin. As can be seen in **Figure 4C**, there is clear evidence that both the tag cleavage and resin binding were highly effective. Moreover, this last step of separation purified the protein even further, as seen in lane 3, where only the final bands of the construct remain, compared to lane 1, where impurities are evident and also to lane 2, where many of these impurifying proteins are bound on the resin. However, in the purification process some degradation occurred. Thus, the final cytotoxic protein with >95% purity is represented by the two clear bands in the supernatant (**Figure 4C**, lane 3). Almost all the impurifying proteins were bound on the resin, or precipitated (lane 2). The final yield of >95% pure Aff-MAG2 obtained was ~12 mg/L of bacterial culture, a most promising yield, given the fact that the resulting untagged protein has a molecular weight 2.4 times lower than the expressed full-length construct (Vasilescu et al., 2025). To clarify, the reported yield was calculated by first determining the concentration of purified Aff-MAG2 protein in the eluate, using the Pierce 660 assay. This concentration was multiplied by the total elution volume to obtain the total amount of protein in milligrams. The final yield was then calculated by dividing this amount by the initial volume of *E. coli* culture (in liters). Thus, pure Aff-MAG2 was obtained for the downstream cell-based experiments. Its amino acid sequence was then validated through nanoLC-MS/MS and the degradation observed was investigated further.

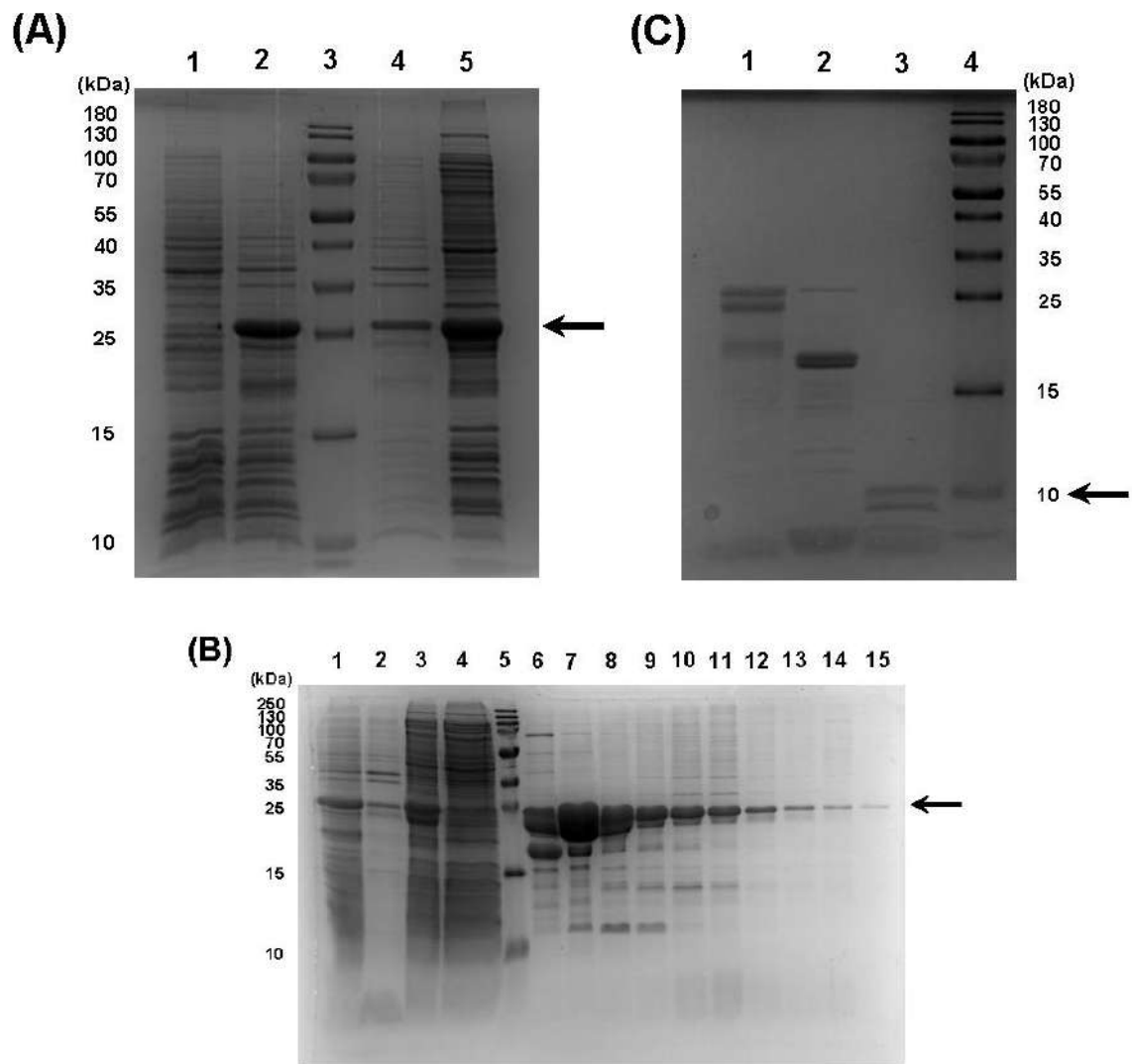


**Figure 4.** Expression and purification of the recombinant AffDC. **(A)** 6xHis-SUMO-Aff-MAG2 expression and solubility. **1** - non-induced bacterial culture, **2** - induced culture, **3** - molecular weight marker, **4** - insoluble fraction from lysed induced bacteria, **5** - soluble fraction from lysed induced bacteria. The black arrow indicates the recombinant fusion protein. **(B)** 6xHis-SUMO-Aff-MAG2 purification. **1** - induced culture, **2** - lysate insoluble fraction, **3** - supernatant from lysate, **4** - purification column flowthrough, **5** - molecular weight marker, **6-15** - eluted fractions in the range 35-67, as seen on chromatogram. The black arrow indicates the recombinant construct. **(C)** Recombinant protein tag cleavage and separation. **1** - negative control reaction - purified recombinant construct without Ulp1, **2** - protein bound to resin, **3** - supernatant with unbound protein, **4** - molecular weight marker. The black arrow indicates untagged Aff-MAG2. This figure is from (Vasilescu et al., 2025), used under the CC BY 4.0 license (<https://creativecommons.org/licenses/by/4.0/>).

## Evaluation of Aff-MAG2 Stability and potential Degradation sites

After purifying the recombinant protein, some degradation was observed, evident in **Figure 4C**. The cause for this and the location of the Aff-MAG2 cleavage were unclear. To determine if the construct degraded over time, a stability test under simulated physiological conditions was employed. Band densitometry analysis was performed on the SDS-PAGE image shown as **Figure 5** and the quantified conversion of the upper band into the lower band demonstrates that Aff-MAG2 has a half-life of ~24 hours in cell culture medium supplemented with serum at 37 °C (lane 3, 50% conversion). This result supports its stability under simulated physiological conditions and indicates that the previously observed degradation was probably a one-time event, occurring during the purification procedure.

Therefore, the hypothesis that emerged was that, because the affibody and the linker are known to be highly stable, the protein was most likely cleaved in the MAG2 region during purification. Given the distance of migration in the gel between the two resulting bands (~2 kDa), it seemed that MAG2 was cleaved just at its N-terminus. NanoLC-MS/MS was utilized to confirm this hypothesis.

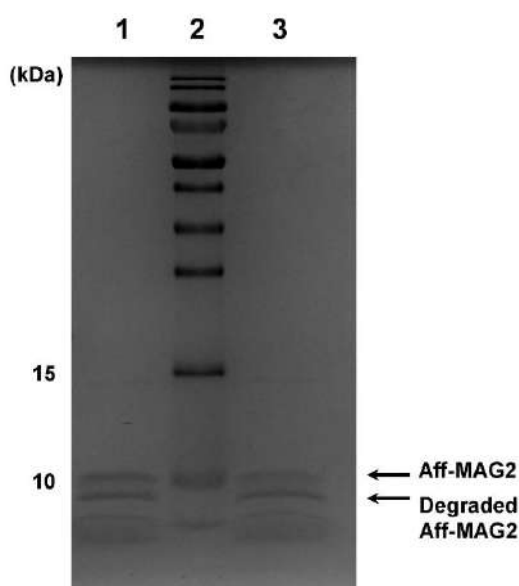


**Figure 5.** SDS-PAGE for the stability of Aff-MAG2 over time at 37 °C. Purified Aff-MAG2 redissolved in previously described cell culture medium with added FBS was incubated for 24 hours at 37 °C. **1** – purified stock Aff-MAG2, **2** – molecular weight marker, **3** – Aff-MAG2 in medium supplemented with serum after incubation. The arrows show full-length Aff-MAG2 and degraded Aff-MAG2, respectively. This figure is from (Vasilescu et al., 2025), used under the CC BY 4.0 license (<https://creativecommons.org/licenses/by/4.0/>).

## **Inhibitory Effect Displayed by Aff-MAG2 on Acute Myeloid Leukemia cells**

After the recombinant compound was purified, validated and its stability was characterized, the next step was to test whether it could inhibit the viability of AML cells in a specific, directed way, given its affibody part with high affinity for B7-H3. The THP-1 cell line was chosen as a classic model for AML. To this end, both THP-1 and RAJI cells were treated with a serial dilution of Aff-MAG2, comprised of the following final concentrations: 1.56  $\mu\text{M}$ , 3.12  $\mu\text{M}$ , 6.25  $\mu\text{M}$ , 12.5  $\mu\text{M}$ , 25  $\mu\text{M}$ , 50  $\mu\text{M}$  and 100  $\mu\text{M}$ , respectively. All treatments were performed for 6 hours, in technical triplicate, followed by MTS assay. RAJI cells represented the negative control for specificity of the cytotoxic product. The technical negative controls for the assay consisted of cells from both lines incubated with only the complete growth medium, without added antibiotics (untreated cells). As the hypothesized mechanism of action of the tested conjugate is permeabilization of the cell membrane, eventually leading to pore formation, the technical positive control utilized for the assay was a 15-minute treatment with Triton X-100 0.02%.

As shown in **Figure 6A**, Aff-MAG2 inhibited THP-1 cell viability in a dose-dependent manner. Conversely, RAJI cell viability remained unaffected at all tested concentrations. For instance, the difference in mean percent viability between the 25  $\mu\text{M}$  and 50  $\mu\text{M}$  treatments in RAJI cells was not statistically significant ( $p > 0.05$ ; **Figure 6B**). In contrast, the nonspecific Triton X-100 caused strong inhibition of RAJI cells as a general permeabilization agent, even when compared to the 100  $\mu\text{M}$  Aff-MAG2 treatment ( $p < 0.001$ , **Figure 6B**), strengthening the hypothesis that the effect of the developed compound is specific to B7-H3<sup>+</sup> cells. The difference in inhibition between RAJI and THP-1 cells was statistically significant at 25  $\mu\text{M}$  ( $p < 0.01$ ) and highly significant at 50  $\mu\text{M}$  and 100  $\mu\text{M}$  ( $p < 0.001$ ), as shown in **Figure 6B**. The calculated half-maximal inhibitory concentration ( $\text{IC}_{50}$ ) of Aff-MAG2 against THP-1 (B7-H3<sup>+</sup>) cells is 26.35  $\mu\text{M}$ , while for RAJI (B7-H3<sup>-</sup>) cells  $\text{IC}_{50}$  is  $> 100 \mu\text{M}$ , a 3-fold or more difference. In conclusion, these data strongly suggest that Aff-MAG2 has a potent and highly specific inhibitory effect against B7-H3-expressing AML cells.

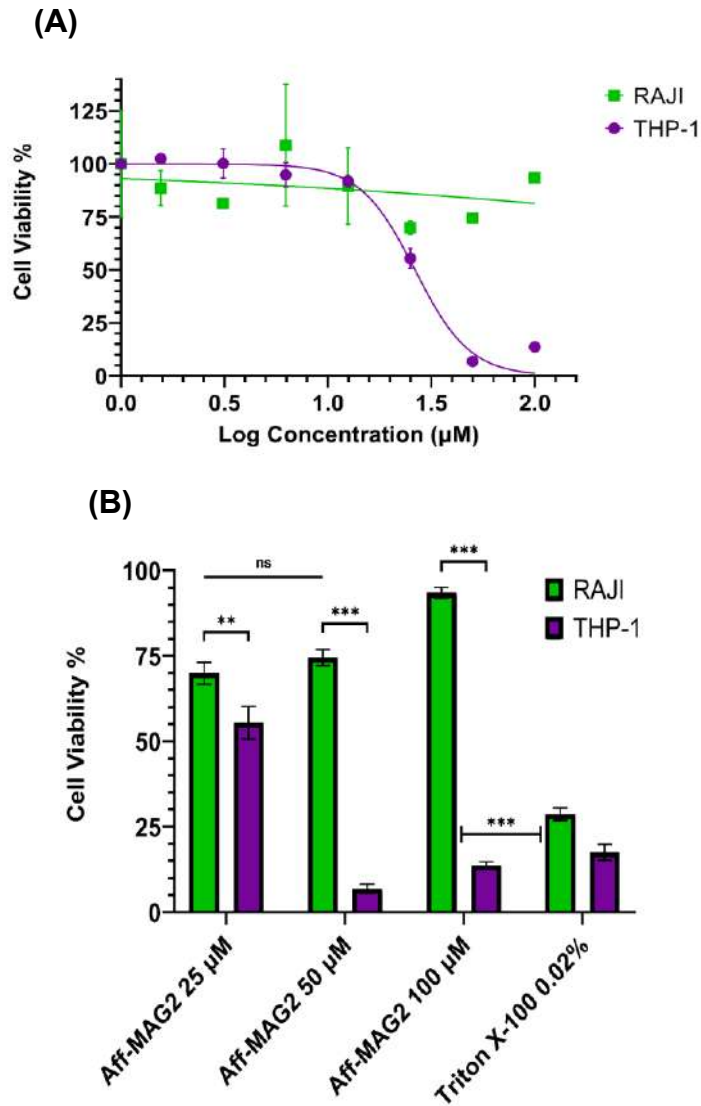


**Figure 6.** MTS assay of AML cells treated with Aff-MAG2. **THP-1 (B7-H3<sup>+</sup>)** and **RAJI (B7-H3<sup>-</sup>)** cells were treated with various concentrations of Aff-MAG2 for 6 hours. **(A)** Inhibitory dose-response curves. The points on both curves represent, in order from left to right, mean percentage cell viability, normalized to untreated cells, at the following concentrations of AffDC compound: 0 μM, 1.56 μM, 3.12 μM, 6.25 μM, 12.5 μM, 25 μM, 50 μM and 100 μM, respectively. **(B)** Pairwise comparison analysis of the MTS assay data between mean percent viability of RAJI and THP-1 cells respectively, normalized to untreated cells, for treatment with 25 μM, 50 μM and 100 μM of Aff-MAG2, respectively. Triton X-100 0.02% - positive control for membrane permeabilization. Error bars represent ±SD,  $n=3$  (technical replicates) from a representative experiment. Unpaired one-tailed  $t$ -test, **ns**  $p \geq 0.05$ , **\*\***  $p < 0.01$ , **\*\*\***  $p < 0.001$ . This figure is adapted from (Vasilescu et al., 2025), used under the CC BY 4.0 license (<https://creativecommons.org/licenses/by/4.0/>).

## **Aff-MAG2 Causes intense Necrosis and Apoptosis in AML cells**

Based on the encouraging results of the MTS assay, the author ventured to investigate the specific effects of the cytotoxic compound on cell function by flow cytometry. First, the cell lines were evaluated for surface expression of the B7-H3 marker. **Figure 7** panels **A**, **B** and **C** show the gating strategy utilized for B7-H3 expression analysis in THP-1, as a representative example. **Figure 7D** shows the flow cytometry validation of the cell models used in this study. As shown, RAJI cells exhibited no surface expression of B7-H3, confirming their suitability as a negative control. On the other hand, THP-1 displayed high B7-H3 surface expression, therefore being an optimal model for validating the developed AffDC.

For the functional studies, THP-1 and RAJI cells were treated with 30  $\mu$ M of compound for 6 hours. **Figure 8** presents results from a representative flow cytometry apoptosis experiment. RAJI cells served as the negative control for specificity, while untreated cells from both lines constituted the technical negative controls. The technical positive control for necrosis was treatment for 15 minutes with Triton X-100 0.02%, while for apoptosis it was an 18-hour treatment with 30  $\mu$ M Cisplatin. In **Figure 8** panels **A**, **B** and **C** is the gating strategy for delimiting the populations of interest.

Strengthening the MTS results, THP-1 cells were highly affected by Aff-MAG2 treatment, showing a viability decrease of approximately 60%, down to 36.18% (lower left quadrant, Annexin V<sup>-</sup>, PI<sup>-</sup>), with 31.37% necrotic (upper right quadrant, Annexin V<sup>+</sup>, PI<sup>+</sup>) and 32.13% apoptotic cells (lower right quadrant, Annexin V<sup>+</sup>, PI<sup>-</sup>), respectively, compared to untreated cells (**Figure 8E**). Oppositely, RAJI cell viability remained unaffected by the treatment (**Figure 8D**). Thus, flow cytometry demonstrates the highly specific necrotic and apoptotic effects Aff-MAG2 has against AML cells. Moreover, the high proportion of necrotic cells among the treated THP-1 suggests a potent membranolytic effect, likely attributable to the Magainin-2 moiety of the recombinant construct.

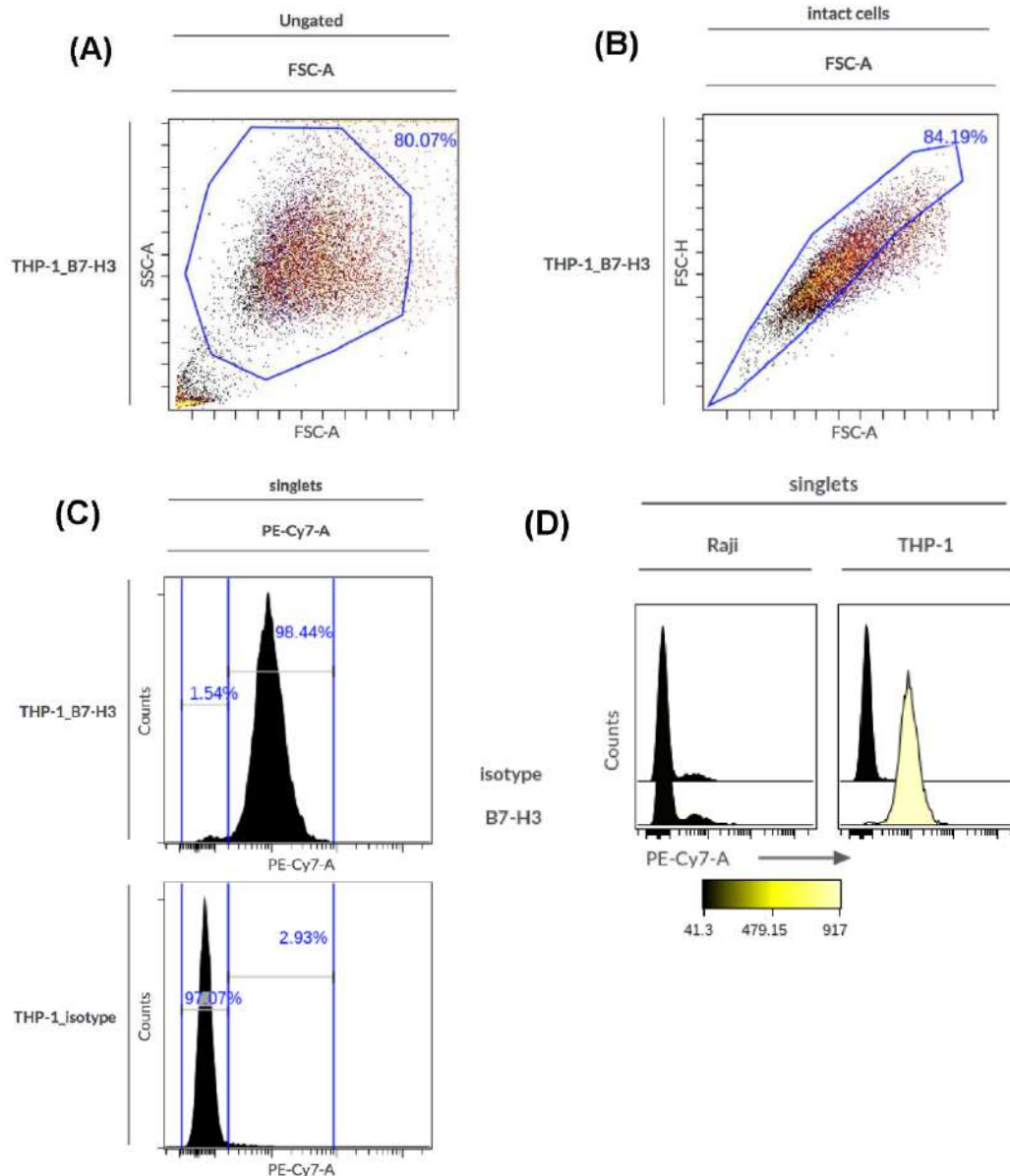


**Figure 7.** Representative examples of the gating strategy for THP-1 cells and flow cytometry analysis of B7-H3 surface expression in RAJI and THP-1 cells. **(A)** FSC-A vs. SSC-A gating for intact cells. **(B)** FSC-A vs. FSC-H singlets gating. **(C)** B7-H3 positive/negative histogram gate based on PE-Cy7 fluorescence, containing anti-B7-H3 antibody and isotype control-labeled cells, respectively. **(D)** Cell surface expression of the B7-H3 ligand. The corresponding antibody utilized for staining is shown on the left side. This figure is adapted from (Vasilescu et al., 2025), used under the CC BY 4.0 license (<https://creativecommons.org/licenses/by/4.0/>).

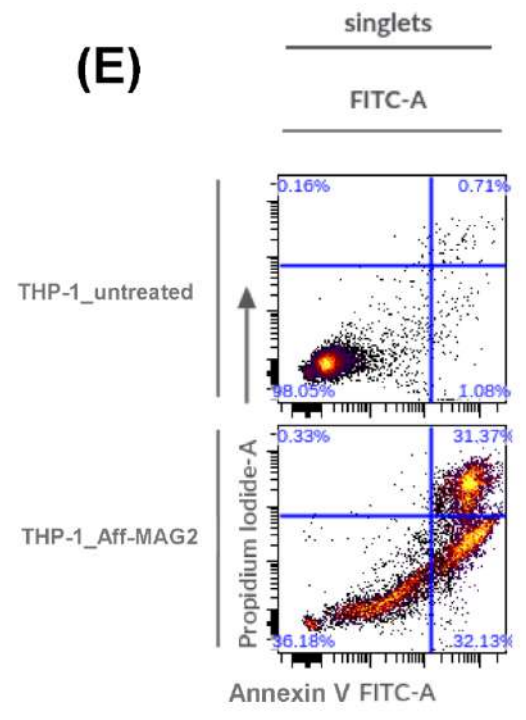
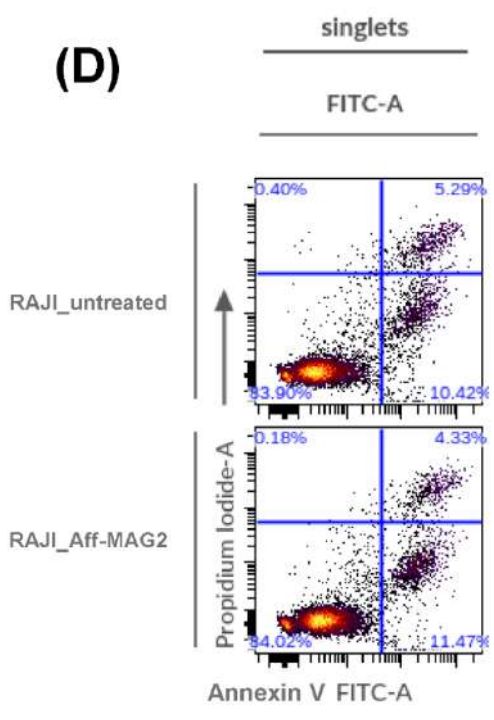
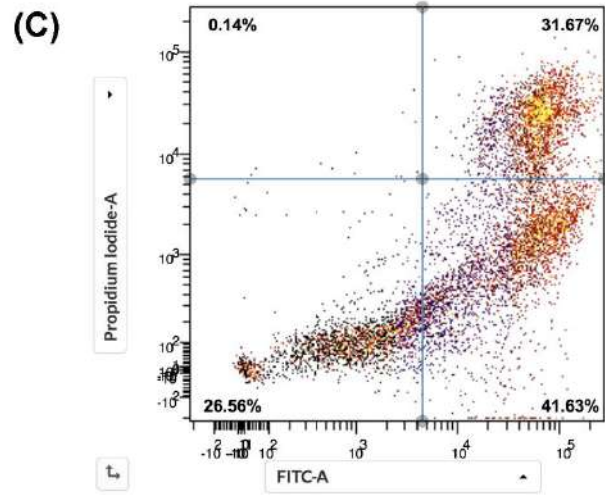
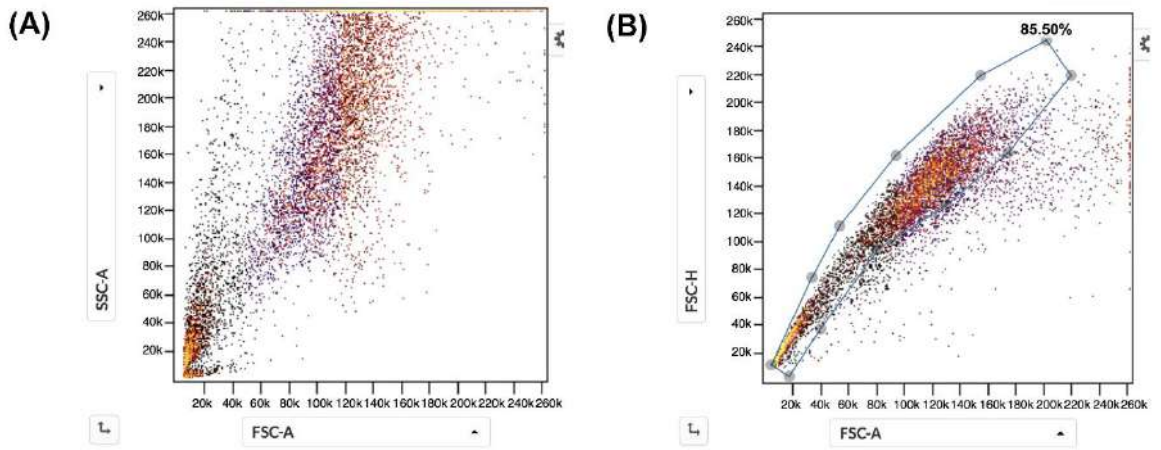


**Figure 8.** Flow cytometry evaluation of necrosis and apoptosis in AML cells treated with Aff-MAG2. Panels (A), (B) and (C) comprise the employed gating strategy, exemplified in the case of THP-1 cells treated with the AffDC. In panels (D) and (E), Aff-MAG2 - treatment with 30  $\mu$ M cytotoxic protein for 6 hours. (A) Ungated cells. (B) Singlets gate. (C) Cell viability, necrosis and apoptosis gate on singlet cells. (D) Necrosis and apoptosis of treated vs. untreated RAJI cells. (E) Necrosis and apoptosis of treated vs. untreated THP-1 cells. Data shown from a representative experiment. This figure is adapted from (Vasilescu et al., 2025), used under the CC BY 4.0 license (<https://creativecommons.org/licenses/by/4.0/>).

### **AML cells Suffer Proliferation Decrease upon treatment with Aff-MAG2**

Finally, the author tested whether the targeted cytotoxin that was developed had any effect on cell proliferation. In a similar experiment to ones previously described in this work, THP-1 and RAJI cells (experimental negative control) were treated with 15  $\mu$ M of purified conjugate for 6 hours, followed by cell harvesting for Western blot analysis. As before, the technical negative controls were the respective cell lines incubated with only complete medium without antibiotics. As **Figure 9** shows, Aff-MAG2 markedly and specifically decreased proliferation of treated THP-1 cells, as only in this group, the proliferation marker Ki-67 (Bading et al., 1989) was not detected (lane 3), compared to untreated cells and the control group, RAJI. The opposite is true for Cleaved Caspase 3, which is a recognized biomarker that initiates both the extrinsic and intrinsic apoptosis pathways (Nicholson et al., 1995). This marker was not detected in any experimental condition, except for treated THP-1 cells (lane 3), which underlines that the majority of these cells underwent apoptosis. On the other hand, RAJI were unaffected by the treatment. These results support the MTS and flow cytometry data, underlining the potency and specificity of the developed compound.

Also, B7-H3 expression patterns were again validated through Western blot (**Figure 9**), as only in THP-1 cells, treated (lane 3) and untreated (lane 1) there was a band for this protein, compared to RAJI, which displayed no signal (lanes 5 and 7). Although it can be seen from the  $\alpha$ -Tubulin loading control that all samples were loaded in equal amounts, the loading control could not be detected in treated THP-1 cells (lane 3). This is probably due to the fact that these cells suffered extensive membrane damage and therefore lost most cytosolic content in the cell medium, which cannot feasibly be recovered. The same is true

for other standard loading controls, like GAPDH, which was also lost from the sample and could not be detected. Nonetheless, lane 3 contains the same amount of total protein, as evidenced by the presence of Cleaved Caspase 3, but also B7-H3, which is a membrane protein and could be recovered through centrifugation. All in all, these data prove that Aff-MAG2 decreases proliferation and increases apoptosis of only THP-1 (B7-H3<sup>+</sup>) AML cells, adding to the observed cumulative effects of this potent, specific and novel protein dual construct (Vasilescu et al., 2025).

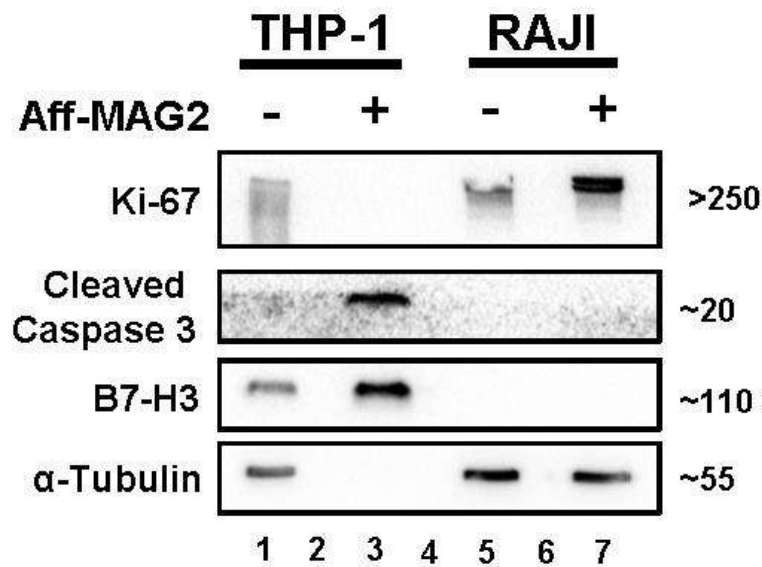


**Figure 9.** Western blot showing proliferation and apoptosis levels in AML cells treated with Aff-MAG2. All samples were total cell lysates, loaded in equal amounts. **Aff-MAG2** - treatment with 15  $\mu$ M AffDC for 6 hours, - untreated cells, + treated cells. The numbers on the right side of the image show the approximate mass in kDa at which the corresponding proteins migrated. Lanes 2 and 6 - empty, lane 4 - molecular weight marker.  $\alpha$ -Tubulin, the loading control, was not detected in lane 3 (treated THP-1 cells). **Ki-67** - established marker for cell proliferation, **Cleaved Caspase 3** - biomarker for all apoptosis pathways. Data from a representative experiment. This figure is adapted from (Vasilescu et al., 2025), used under the CC BY 4.0 license (<https://creativecommons.org/licenses/by/4.0/>).

### 3. DISCUSSION

This work aimed to design, develop and evaluate *in cellulo* an innovative Affibody-Cytotoxin recombinant protein with specific cytotoxic properties against B7-H3-overexpressing AML cells. Thus, the construct developed in this study is envisioned to address the dire need for personalized therapy of AML patients (please also see **PART I., section 1.**). This AffDC is composed of an Affibody with high affinity against B7-H3 that was previously demonstrated (Oroujeni et al., 2023) (please also see **PART I., section 2.**) coupled to Magainin-2, a strong membranolytic cytotoxic peptide with proven lethality against tumor cells (Lehmann et al., 2006) (please also see **PART I., section 3.**). The fusion protein was designed for high-level soluble expression in *E. coli* and subsequently purified by IMAC. Thanks to this detailed strategy, pure Aff-MAG2 was obtained in high yields and its amino acid sequence was subsequently confirmed through nanoLC-MS/MS. In addition, the AffDC proved stable in simulated physiological conditions.

This study hereby reports that the compound's  $IC_{50}$  of 26.35  $\mu\text{M}$  against THP-1 cells is approximately 3-fold smaller than the 75.2  $\mu\text{M}$  observed against bladder cancer cells for simple Magainin-2 (Lehmann et al., 2006) and over 2-fold smaller than the  $>60 \mu\text{M}$  reported by another group in 1991 (Cruciani et al.) on several tumor cell lines from the hematopoietic lineage, again using the simple peptide. To the author's knowledge, the only study that reported lower  $IC_{50}$  values than the present one ( $\sim 8 \mu\text{M}$ ), performed on lung cancer cell lines by Ohsaki et al. (1992), employed synthetic analogues of MAG2 in a treatment that lasted 4 days, compared to the 6-hour treatment in this study. Thus, it is possible that the increased toxic effect on treated cells was caused by the longer incubation time. More importantly, these analogues presented an  $IC_{50}$  on normal human fibroblasts in the approximate range 21 to 29  $\mu\text{M}$ . This reveals much more aggressive collateral effects on normal cells, with a smaller difference from the activity threshold on malignant cells, than for Aff-MAG2 ( $IC_{50}$  against RAJI  $>100 \mu\text{M}$ ). Therefore, compared to previously reported data on the off-target toxicity of MAG2 analogues on fibroblasts, this study presents a favorable selectivity window for AML cells that are B7-H3-positive, as demonstrated by the resistance to Aff-MAG2 of RAJI cells. This resistance manifests in spite of RAJI cells being tumoral. Thus, the developed targeted cytotoxic molecule has much higher specificity to B7-H3<sup>+</sup> AML cells and possesses considerably less off-target effects than the toxin alone, or its derivatives.

Also, to the author's knowledge, this study is one of the very few that evaluates the Magainin-2 toxin on AML cells, bringing novelty to the approached disease as well (Vasilescu et al., 2025).

With the promise of hopeful clinical trials against B7-H3-positive cancers, such as that on the radioactive monoclonal antibody (mAb) <sup>131</sup>I-omburtamab on neuroblastoma patients (Kramer et al., 2022), or Chimeric Antigen Receptor (CAR)-T cells with single-chain variable fragments (scFvs) directed against B7-H3 in a multitude of solid and liquid malignancies that significantly outperform mAbs (Guo et al., 2025), it is increasingly convincing that this antigen is a target of high importance for personalized medicine. For this reason, in this work, the author developed a novel B7-H3-directed cytotoxic vehicle which can be produced in *E. coli* with high yield and cost-efficiency, utilizing simple genetic engineering, with no requirements for cumbersome chemical modifications. It is very small, highly soluble and does not need a delivery system to cancer cells. Furthermore, Aff-MAG2 targets B7-H3-expressing AML cells selectively, with strong lethal effects and little to no off-site damage, making it a candidate that holds great promise for future personalized AML therapy.

## **Limitations**

The main limitations of this study include partial degradation of the recombinant protein during purification and the challenge of identifying a suitable loading control for Western blot that is retained consistently by the treated cells which express B7-H3. Additionally, there was no *in vivo* testing of the stability and effects of Aff-MAG2, to evaluate its potential properly in a closer environment to the clinical one.

## **Perspectives**

To address these limitations, future studies will focus on stabilization of Aff-MAG2 to prevent degradation and on employing more resilient B7-H3-negative cell lines for comparative testing. Also, other biochemistry and *in cellulo* techniques, including microscopy, will be utilized to characterize the compound's pharmacokinetic properties and mechanism of action. Moving forward, an *in vivo* pre-clinical study will be employed to test the efficiency of this novel anti-tumoral compound in patient-derived xenograft models for AML.

### III. CONCLUSION

Taken together, the results obtained using AML representative B7-H3-positive THP-1 and B7-H3-negative RAJI cells demonstrate that the cytotoxic Aff-MAG2 molecule developed exhibits strong necrotic, apoptotic and antiproliferative activity, highly specific to B7-H3-positive AML cells, with almost no collateral effects. Moreover, this observed activity is significantly stronger than the previously reported effects of Magainin-2 alone. In conclusion, the author designed, produced and evaluated a novel Anti-B7-H3 Cytotoxic Affibody that from the *in vitro* data, demonstrates high potential for further pre-clinical and *in vivo* studies and ultimately, translation to AML personalized therapy.

### ACKNOWLEDGEMENTS

This work was supported by the Romanian Academy through the Doctoral School of Advanced Studies. This research did not receive dedicated financial support for the purchase of reagents from commercial, public, or not-for-profit funding agencies. A Fulbright Visiting Scholar grant (No. 779/14.06.2022) awarded to Prof. Dr. Ștefan-Eugen Szedlacsek supported in part the conceptual development of the study. Additionally, the nanoLC-MS/MS analysis was partly supported by the grant of the Ministry of Research, Innovation and Digitization, CNCS - UEFISCDI, project number PN-IV-P8-8.3-ROMD-2023-0100, Contract 25ROMD/2024. Also, the Bilateral Collaboration between the Romanian Academy and the Hungarian Academy, with project number 2286/15.09.2021, between 2022-2024, titled “Radiolabelling of affibody for tumor diagnostic and theranostic application in the nuclear medicine” supported the collaborative work for the already mentioned secondary article at the basis of this thesis, (Váradi et al., 2023). I warmly thank Dr. Adrian Bogdan Țigu from the Research Centre for Advanced Medicine–MEDFUTURE at Iuliu Hațieganu University of Medicine and Pharmacy, Cluj-Napoca, Romania, for kindly providing the RAJI cells and the Viral Glycoproteins Department of the Institute of Biochemistry of the Romanian Academy for providing the anti- $\alpha$ -Tubulin antibody. The funders had no involvement in the conceptualization or experimental planning of this thesis.

## LIST OF PUBLICATIONS

1. **Vasilescu, A.-M.**, Vasilescu, A.-G., Sima, L. E., Munteanu, C. V. A., Baran, N. & Szedlacsek, Ş.-E. 2025. A novel cytotoxic anti-B7-H3 affibody with therapeutic potential in acute myeloid leukemia. *Front. Pharmacol.* 16:1684226. DOI: 10.3389/fphar.2025.1684226.
2. Váradi, B., Brezovcsik, K., Garda, Z., Madarasi, E., Szedlacsek, H., Badea, R.-A., **Vasilescu, A.-M.**, Puiu, A.-G., Ionescu, A. E., Sima, L.-E., Munteanu, C. V. A., Călăraş, S., Vágner, A., Szikra, D., Toàn, N. M., Nagy, T., Szűcs, Z., Szedlacsek, S., Nagy, G. & Tirscó, G. 2023. Synthesis and characterization of a novel [<sup>52</sup>Mn]Mn-labelled affibody based radiotracer for HER2+ targeting. *Inorg. Chem. Front.* 10. 4734– 4745. DOI: 10.1039/D3QI00356F.
3. Vasilescu, A.-G., **Vasilescu, A.-M.**, Sima, L. E., Baran, N. & Szedlacsek, Ş.-E. 2025. Breaking the cancer code: a novel DNA minicircle to disable STAT3 in ovarian cancer cells SKOV3. *Front. Pharmacol.* 16:1673427. DOI: 10.3389/fphar.2025.1673427.
4. **Vasilescu, A.**, Puiu, A., Szedlacsek, S. 2025. A novel cytotoxic fusion protein targeting B7-H3 for acute myeloid leukemia therapy. *FEBS Open Bio.* 15:P-32-103. DOI: 10.1002/2211-5463.70071. - Poster presented during *The 49<sup>th</sup> FEBS Congress, Istanbul, 2025.*
5. Puiu, A., **Vasilescu, A.**, Szedlacsek, S. 2025. Development of a novel small circular DNA decoy inhibitor targeting STAT3 for cancer therapy. *FEBS Open Bio.* 15:P-32-102. DOI: 10.1002/2211-5463.70071. - Poster presented during *The 49<sup>th</sup> FEBS Congress, Istanbul, 2025.*
6. Váradi, B., Garda, Z., Madarasi, E., Brezovcsik, K., Vágner, A., Nagy, T., Garai, I. M., Puiu, A. G., **Vasilescu, A. M.**, Szűcs, Z., Szedlacsek, S. E., Nagy, G., Tirfél, Gy. 2022. Labeling of anti-HER2-affibodies with <sup>52</sup>Mn via pyclen-based bifunctional ligands: from ligand design to in vivo PET/MR experiments. - Poster presented during *The 35<sup>th</sup> Annual Congress of the European Association of Nuclear Medicine, Barcelona, 2022.*

## REFERENCES

1. Abramson, J., Adler, J., Dunger, J., Evans, R., Green, T., Pritzel, A., Ronneberger, O., Willmore, L., Ballard, A. J., Bambrick, J., Bodenstein, S. W., Evans, D. A., Hung, C. C., O'Neill, M., Reiman, D., Tunyasuvunakool, K., Wu, Z., Žemgulytė, A., Arvaniti, E., ... Jumper, J. M. (2024). Accurate structure prediction of biomolecular interactions with AlphaFold 3. *Nature*, *630*(8016), 493–500. <https://doi.org/10.1038/s41586-024-07487-w>
2. ATCC: The Global Bioresource Center. (n.d.). Retrieved July 1, 2025, from <https://www.atcc.org/>
3. Bading, H., Rauterberg, E. W., & Moelling, K. (1989). Distribution of c-myc, c-myb, and Ki-67 Antigens in Interphase and Mitotic Human Cells Evidenced by Immuno-fluorescence Staining Technique. In *Experimental Cell Research* (Vol. 185).
4. Baker, M. A., Maloy, W. L., Zasloff, M., & Jacob, L. S. (1993). Anticancer Efficacy of Magainin2 and Analogue Peptides. *Cancer Research*, *53*, 3052–3057. <http://aacrjournals.org/cancerres/article-pdf/53/13/3052/2450843/cr0530133052.pdf>
5. Bommarius, B., Janssen, H., Elliott, M., Kindrachuk, J., Pasupuleti, M., Gieren, H., Jaeger, K. E., Hancock, R. E. W., & Kalman, D. (2010). Cost-effective expression and purification of antimicrobial and host defense peptides in *Escherichia coli*. *Peptides*, *31*(11), 1957–1965. <https://doi.org/10.1016/j.peptides.2010.08.008>
6. Chen, X., Zaro, J. L., & Shen, W. C. (2013). Fusion protein linkers: Property, design and functionality. In *Advanced Drug Delivery Reviews* (Vol. 65, Issue 10, pp. 1357–1369). <https://doi.org/10.1016/j.addr.2012.09.039>
7. Cheng, J., Randall, A. Z., Sweredoski, M. J., & Baldi, P. (2005). SCRATCH: A protein structure and structural feature prediction server. *Nucleic Acids Research*, *33*(SUPPL. 2). <https://doi.org/10.1093/nar/gki396>
8. Cruciani, R. A., Barker, J. L., Zasloff, M., Chen, Hao.-C., & Colamonici, O. (1991). Antibiotic magainins exert cytolytic activity against transformed cell lines through channel formation. *Proc. Natl. Acad. Sci. USA*, *88*, 3792–3796.

9. Fan, S., Wang, T., You, F., Zhang, T., Li, Y., Ji, C., Han, Z., Sheng, B., Zhai, X., An, G., Meng, H., & Yang, L. (2023). B7-H3 chimeric antigen receptor-modified T cell shows potential for targeted treatment of acute myeloid leukaemia. *European Journal of Medical Research*, 28(1). <https://doi.org/10.1186/s40001-023-01049-y>
10. Gasteiger, E., Hoogland, C., Gattiker, A., Duvaud, S., Wilkins, M. R., Appel, R. D., & Bairoch, A. (2005). Protein Identification and Analysis Tools on the ExPASy Server. In J. M. Walker (Ed.), *The Proteomics Protocols Handbook* (pp. 571–607). Humana Press. <http://www.expasy.org/tools/>.
11. Goldman, M. J., Craft, B., Hastie, M., Repečka, K., McDade, F., Kamath, A., Banerjee, A., Luo, Y., Rogers, D., Brooks, A. N., Zhu, J., & Haussler, D. (2020). Visualizing and interpreting cancer genomics data via the Xena platform. In *Nature Biotechnology* (Vol. 38, Issue 6, pp. 675–678). Nature Research. <https://doi.org/10.1038/s41587-020-0546-8>
12. Guo, Y., Wang, X., Zhang, C., Chen, W., Fu, Y., Yu, Y., Chen, Y., Shao, T., Zhang, J., & Ding, G. (2025). Tumor Immunotherapy Targeting B7-H3: From Mechanisms to Clinical Applications. In *ImmunoTargets and Therapy* (Vol. 14, pp. 291–320). Dove Medical Press Ltd. <https://doi.org/10.2147/ITT.S507522>
13. Kramer, K., Pandit-Taskar, N., Kushner, B. H., Zanzonico, P., Humm, J. L., Tomlinson, U., Donzelli, M., Wolden, S. L., Haque, S., Dunkel, I., Souweidane, M. M., Greenfield, J. P., Tickoo, S., Lewis, J. S., Lyashchenko, S. K., Carrasquillo, J. A., Chu, B., Horan, C., Larson, S. M., ... Modak, S. (2022). Phase 1 study of intraventricular 131I-omburtamab targeting B7H3 (CD276)-expressing CNS malignancies. *Journal of Hematology and Oncology*, 15(1). <https://doi.org/10.1186/s13045-022-01383-4>
14. Lehmann, J., Retz, M., Sidhu, S. S., Suttman, H., Sell, M., Paulsen, F., Harder, J., Unteregger, G., & Stöckle, M. (2006). Antitumor Activity of the Antimicrobial Peptide Magainin II against Bladder Cancer Cell Lines. *European Urology*, 50(1), 141–147. <https://doi.org/10.1016/j.eururo.2005.12.043>
15. Li, Y. (2011). Recombinant production of antimicrobial peptides in *Escherichia coli*: A review. *Protein Expression and Purification*, 80(2), 260–267. <https://doi.org/10.1016/j.pep.2011.08.001>

16. Matsuzaki, K. (1998). Magainins as paradigm for the mode of action of pore forming polypeptides. *Biochimica et Biophysica Acta (BBA) - Reviews on Biomembranes*, 1376(3), 391–400. [https://doi.org/10.1016/S0304-4157\(98\)00014-8](https://doi.org/10.1016/S0304-4157(98)00014-8)
17. Nicholson, D. W., Ali, A., Thornberry, N. A., Vaillancourt, J. P., Ding, C. K., Gallant, M., Gareau, Y., Griffin, P. R., Labelle, M., Lazebnik, Y. A., Munday, N. A., Raju, S. M., Smulson, M. E., Yamin, T. T., Yu, V. L., & Miller, D. K. (1995). Identification and inhibition of the ICE/CED-3 protease necessary for mammalian apoptosis. *Nature*, 376(6535), 37–43. <https://doi.org/10.1038/376037A0>
18. Ohsaki, Y., Gazdar, A. F., Chen, H.-C., & Johnson, B. E. (1992). Antitumor Activity of Magainin Analogues against Human Lung Cancer Cell Lines. *Cancer Research*, 52, 3534–3538. <http://aacrjournals.org/cancerres/article-pdf/52/13/3534/2448103/cr0520133534.pdf>
19. Oroujeni, M., Bezverkhniaia, E. A., Xu, T., Liu, Y., Plotnikov, E. V., Klint, S., Ryer, E., Karlberg, I., Orlova, A., Frejd, F. Y., & Tolmachev, V. (2023). Evaluation of affinity matured Affibody molecules for imaging of the immune checkpoint protein B7-H3. *Nuclear Medicine and Biology*, 124–125. <https://doi.org/10.1016/j.nucmedbio.2023.108384>
20. Pandidan, S., & Mechler, A. (2025). Nano-viscosimetry analysis of membrane disrupting peptide magainin2 interactions with model membranes. *Biophysical Chemistry*, 318, 107390. <https://doi.org/10.1016/J.BPC.2025.107390>
21. Ramos, R., Moreira, S., Rodrigues, A., Gama, M., & Domingues, L. (2013). Recombinant expression and purification of the antimicrobial peptide magainin-2. *Biotechnology Progress*, 29(1), 17–22. <https://doi.org/10.1002/BTPR.1650>
22. *Scientific Image and Illustration Software | BioRender*. (n.d.). Retrieved October 2, 2025, from <https://www.biorender.com/>
23. Stefańczyk, S. A., Hagelstein, I., Lutz, M. S., Müller, S., Holzmayer, S. J., Jarjour, G., Zekri, L., Heitmann, J. S., Salih, H. R., & Märklin, M. (2024). Induction of NK cell reactivity against acute myeloid leukemia by Fc-optimized CD276 (B7-H3) antibody. *Blood Cancer Journal*, 14(1). <https://doi.org/10.1038/s41408-024-01050-6>
24. Tan, X., & Zhao, X. (2024). B7-H3 in acute myeloid leukemia: From prognostic biomarker to immunotherapeutic target. In *Chinese Medical Journal* (Vol. 137,

- Issue 21, pp. 2540–2551). Lippincott Williams and Wilkins.  
<https://doi.org/10.1097/CM9.0000000000003099>
25. Tolmachev, V., Papalanis, E., Bezverkhniaia, E. A., Rosly, A. H., Vorobyeva, A., Orlova, A., Carlqvist, M., Frejd, F. Y., & Oroujeni, M. (2025). Impact of Radiometal Chelates on In Vivo Visualization of Immune Checkpoint Protein Using Radiolabeled Affibody Molecules. *ACS Pharmacology and Translational Science*. <https://doi.org/10.1021/acsptsci.4c00539>
  26. Tyagi, A., Ly, S., El-Dana, F., Yuan, B., Jaggupilli, A., Grimm, S., Konopleva, M., Bühring, H. J., & Battula, V. L. (2022). Evidence supporting a role for the immune checkpoint protein B7-H3 in NK cell-mediated cytotoxicity against AML. *Blood*, *139*(18), 2782–2796. <https://doi.org/10.1182/blood.2021014671>
  27. Váradi, B., Brezovcsik, K., Garda, Z., Madarasi, E., Szedlaczek, H., Badea, R. A., Vasilescu, A. M., Puiu, A. G., Ionescu, A. E., Sima, L. E., Munteanu, C. V. A., Călăraș, S., Vágner, A., Szikra, D., Toàn, N. M., Nagy, T., Szűcs, Z., Szedlaczek, S., Nagy, G., & Tircsó, G. (2023). Synthesis and characterization of a novel [<sup>52</sup>Mn]Mn-labelled affibody based radiotracer for HER2+ targeting. *Inorganic Chemistry Frontiers*, *10*(16), 4734–4745. <https://doi.org/10.1039/d3qi00356f>
  28. Vasilescu, A.-M., Vasilescu, A.-G., Sima, L. E., Munteanu, C. V. A., Baran, N., & Szedlaczek, Ș.-E. (2025). A novel cytotoxic anti-B7-H3 affibody with therapeutic potential in acute myeloid leukemia. *Frontiers in Pharmacology*, *16*. <https://doi.org/10.3389/fphar.2025.1684226>
  29. Wittwer, N. L., Brumatti, G., Marchant, C., Sandow, J. J., Pudney, M. K., Dottore, M., D'Andrea, R. J., Lopez, A. F., Ekert, P. G., & Ramshaw, H. S. (2017). High CD123 levels enhance proliferation in response to IL-3, but reduce chemotaxis by downregulating CXCR4 expression. *Blood Advances*, *1*(15), 1067–1079. <https://doi.org/10.1182/bloodadvances.2016002931>
  30. Zasloff, M. (1987). Magainins, a class of antimicrobial peptides from *Xenopus* skin: Isolation, characterization of two active forms, and partial cDNA sequence of a precursor. *Proceedings of the National Academy of Sciences of the United States of America*, *84*(15), 5449–5453. <https://doi.org/10.1073/pnas.84.15.5449>
  31. Zhang, Z., Jiang, C., Liu, Z., Yang, M., Tang, X., Wang, Y., Zheng, M., Huang, J., Zhong, K., Zhao, S., Tang, M., Zhou, T., Yang, H., Guo, G., Zhou, L., Xu, J., & Tong, A. (2020). B7-H3-Targeted CAR-T Cells Exhibit Potent Antitumor

Effects on Hematologic and Solid Tumors. *Molecular Therapy Oncolytics*, 17, 180–189. <https://doi.org/10.1016/j.omto.2020.03.019>

32. Zorko, M., & Jerala, R. (2010). Production of Recombinant Antimicrobial Peptides in Bacteria. In A. Giuliani & A. C. Rinaldi (Eds.), *Methods in Molecular Biology* (Vol. 618, pp. 61–75). Humana Press. <https://doi.org/10.1007/978-1-60761-594-1>